





## Article

# The Removal of Phosphorus from Wastewater Using a Sewage Sludge Biochar: A Column Study

Tomas Januševičius <sup>1</sup>, Aušra Mažeikienė <sup>1,\*</sup>, Kateryna Stepova <sup>2</sup>, Vaidotas Danila <sup>1</sup> and Dainius Paliulis <sup>3</sup>

- <sup>1</sup> Research Institute of Environmental Protection, Vilnius Gediminas Technical University, Saulėtekio al. 11, 10223 Vilnius, Lithuania; tomas.janusevicius@vilniustech.lt (T.J.); vaidotas.danila@vilniustech.lt (V.D.)
- <sup>2</sup> Department of Environmental Safety, Lviv State University of Life Safety, 35 Kleparivska str., 79000 Lviv, Ukraine; katyastepova@gmail.com
- <sup>3</sup> Department of Environmental Protection and Water Engineering, Vilnius Gediminas Technical University, Saulėtekio al. 11, 10223 Vilnius, Lithuania; dainius.paliulis@vilniustech.lt
- \* Correspondence: ausra.mazeikiene@vilniustech.lt

**Abstract:** This scientific study investigated the adsorption capabilities of biochar samples derived from municipal sewage sludge pellets. Sewage sludge was pyrolyzed at various temperatures (400, 500, and 600 °C), and the biochar's properties, including specific surface area, pore volume, and pore size distribution, were assessed. The results indicate that the sewage sludge biochar samples are mesoporous materials with significant potential for good adsorption performance. Despite showing a decrease in specific surface area compared to that achieved with pyrolysis at 400 °C, samples pyrolyzed at 600 °C demonstrated an increase in mesopore surface area, enhancing their adsorption potential. Two filtration experiments, conducted at a flow rate of 8 mL/min, revealed that the column containing sewage sludge pyrolyzed at 600 °C retained phosphorus the most effectively during the first and second experiments (with retention efficiencies of 87% and 78%, respectively). The study concludes that municipal sewage sludge biochar could be a promising material for the removal of phosphorus from wastewater and represents a viable solution for sustainable environmental development.

**Keywords:** sewage sludge; pellets; phosphorus; wastewater; adsorption



**Citation:** Januševičius, T.; Mažeikienė, A.; Stepova, K.; Danila, V.; Paliulis, D. The Removal of Phosphorus from Wastewater Using a Sewage Sludge Biochar: A Column Study. *Water* **2024**, *16*, 1104. <https://doi.org/10.3390/w16081104>

Academic Editor: José Alberto Herrera-Melián

Received: 9 March 2024

Revised: 4 April 2024

Accepted: 10 April 2024

Published: 12 April 2024



**Copyright:** © 2024 by the authors. Licensee MDPI, Basel, Switzerland. This article is an open access article distributed under the terms and conditions of the Creative Commons Attribution (CC BY) license (<https://creativecommons.org/licenses/by/4.0/>).

## 1. Introduction

The management of sewage sludge is an international problem. The number of users connected to sewage networks is growing, so there is an increasing need to implement more modern, efficient, and environmentally friendly sludge management technologies in water treatment plants [1]. Among the more modern methods of sludge management are anaerobic digestion, dewatering, and drying. Dried sludge can be used as a biofuel or in agriculture [2]. The chemical composition of the treated sludge determines its further applicability [3]. Sewage sludge generated from residential areas falling within categories I and II can be used as a fertilizer for cultivating cereals, technical crops, and energy forests. Additionally, it is valuable for restoring abandoned lands and can contribute to the recultivation of gravel, sand, or clay quarries. Furthermore, it serves as a means to fertilize urban greenery. Sludge reuse in agriculture often leads to the unintentional accumulation of pollutants in soils, which, under certain circumstances, leach through the soil profile and contaminate the groundwater. Sewage sludge may contain both organic and inorganic contaminants, with metallic elements, particularly heavy metals, being predominant. One of the primary considerations in evaluating the suitability of sewage sludge for agricultural purposes is the heavy metal content. The use of sludge containing heavy metals in agriculture is limited, as an excess of individual elements in the soil may have a toxic effect [4,5]. Zinc, copper, nickel, and cadmium have been found in sewage sludge [3], and these elements can retain phosphate phosphorus (PO<sub>4</sub>-P) [6,7].

As phosphorus is thought to be the main cause of eutrophication, it has recently received much attention [8–10].  $\text{PO}_4\text{-P}$  enters natural waters along with insufficiently treated domestic or surface wastewater. Even very low concentrations of phosphorus (from 0.003 mg/L) can cause the eutrophication of water bodies [11]. Phosphorus can be removed from wastewater using chemical, biological, and physical methods. Chemical methods for P removal from wastewater are widely used because they are generally reliable and effective [12]. Phosphorus is chemically removed from wastewater through sedimentation. This method has the advantages of simple operation and an excellent phosphorus removal effect [13]. Biological methods are widely used to treat wastewater, specifically through the use of activated sludge [14]. Compared to the chemical method, the advantages of biological phosphorus removal are that it is low cost and involves less sludge production [15]. The disadvantages of the first two methods are that the biological method is not effective at low P levels, and the chemical method, which adds soluble Al, Fe, and Ca salts, promotes sludge formation [16]. Additionally, physical techniques such as membrane filters and reverse osmosis are not viable due to their high cost for this specific application [17]. The fact that sorption technology is highly efficient and does not create sludge makes it attractive and practical [10]. The removal of phosphorus from water can be achieved using a variety of sorbents, including biochar [11–16]. This is a type of sustainable carbonaceous substance produced when organic waste streams, including agricultural waste, are thermally treated in the absence of oxygen [11]. Carbonaceous materials like biochar have been employed as effective solid sorbents for soil amendment, phosphorus removal, and carbon capture. The biomass feedstock for producing the biochars can come from spruce [18], reeds [19], sheep manure [20], dairy cow slurry [21], date seed biochar [22], and sewage sludge [23]. Due to its sustainability and low-cost benefits for treating wastewater containing heavy metals, sludge biochar has recently attracted much attention [24]. It has been demonstrated that producing biochar from sewage sludge enables the safe processing of sewage sludge while also yielding an affordable and long-lasting sorbent [25]. The sorbents derived from sewage sludge typically possess a relatively large specific surface area (100–200  $\text{m}^2/\text{g}$ ) and developed microporosity [22].

Previous studies have shown that pyrolyzed sewage sludge is suitable for removing copper, acidic and basic dyes, phenol, phenanthrene, pyrene, and bisphenol A from solutions [26–29]. Hence, it is hypothesized that biochar produced from sewage sludge can effectively remove  $\text{PO}_4\text{-P}$  from wastewater. The aim of this study was to investigate the ability of pyrolyzed sewage sludge to dynamically retain  $\text{PO}_4\text{-P}$ .

## 2. Materials and Methods

### 2.1. Characterization of Adsorbents

Sewage sludge pellets were obtained from the Vilnius city wastewater treatment plant. In the Vilnius wastewater treatment plant, sludge from primary and secondary clarifiers is mixed, thickened by presses, and digested anaerobically in methane tanks. Prior to anaerobic digestion, the sludge is prepared through thermohydrolysis. After anaerobic digestion, the sludge is dewatered and dried to produce pellets.

The moisture content of the obtained sewage sludge pellets was  $4.2 \pm 0.1\%$ . Detailed information regarding the preparation of sewage sludge biochar, as well as its characteristics and composition, is presented in our previous study [30]. Briefly, biochar was derived from sewage sludge pellets through pyrolysis using a muffle furnace. The following sorbents were chosen for sorption studies: PS\_400—sludge pyrolyzed at 400 °C; PS\_500—sludge pyrolyzed at 500 °C; and PS\_600—sludge pyrolyzed at 600 °C. Various pyrolysis temperatures were selected to determine the optimal conditions for sorbent production because the elemental composition, surface area, and porosity of biochars are greatly influenced by the pyrolysis temperature [31,32].

The surface morphology of the prepared sewage sludge biochars (0.6–1.0 mm in size) was analyzed using a scanning electron microscope (SEM), an FEI Helios Nanolab 650 dual beam system equipped with energy-dispersive X-ray spectrometry (EDS) for elemental



analysis. SEM images (at 100 and 10,000 $\times$  magnification) of sewage sludge biochar particles are presented in Figure 1. The micrographs show irregularly shaped particles with rough surfaces characterized by cracks and holes. Notably, pyrolysis at 600  $^{\circ}$ C resulted in the formation of porous structures, evident from the image made at 10,000 $\times$  magnification (Figure 1c).

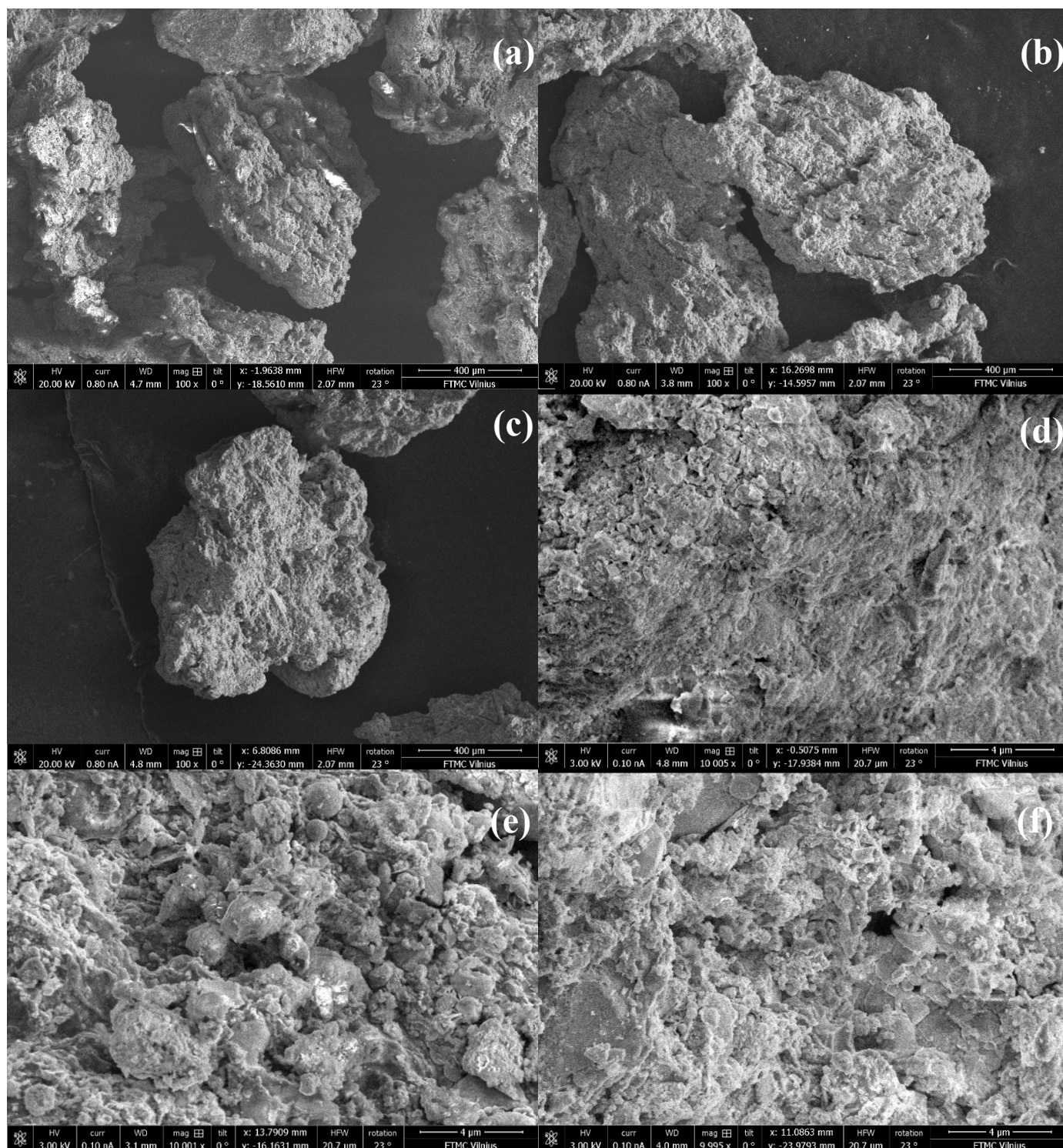


**Figure 1.** SEM images of sewage sludge biochar samples: PS\_400 at 100 $\times$  magnification (a), PS\_500 at 100 $\times$  magnification (b), PS\_600 at 100 $\times$  magnification (c), PS\_400 at 10,000 $\times$  magnification (d), PS\_500 at 10,000 $\times$  magnification (e), and PS\_600 at 10,000 $\times$  magnification (f).

The EDS spectra (Figure 2) show that pyrolyzed sludge (at 400, 500, and 600 °C) mainly contained C, Ca, Si, P, Fe, Al, Mg, and K.

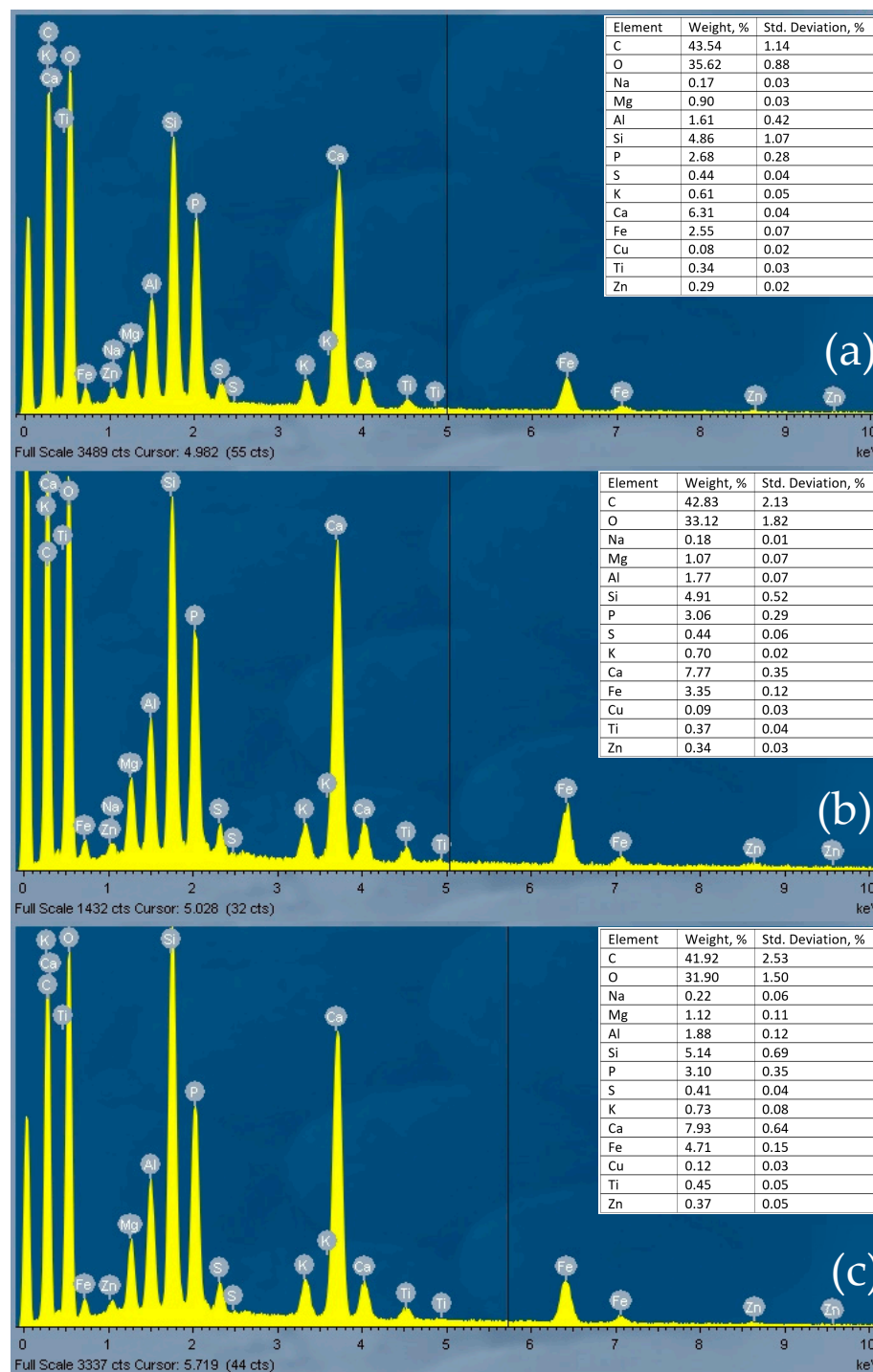


**Figure 2.** EDS spectra of sewage sludge biochars: PS\_400 (a), PS\_500 (b), PS\_600 (c).

The Quantachrome Autosorb-iQ-KR/MP automated high-vacuum gas sorption analyzer, which records nitrogen adsorption/desorption isotherms, was used to determine the specific surface area, pore volume, and pore size distribution of the sludge biochar. Before analysis, samples were outgassed for three hours at 150 °C under vacuum conditions. Nitrogen adsorption and desorption isotherms were then measured at  $-196$  °C (77 °K). The specific surface area was determined using the Brunauer–Emmett–Teller (BET) equation. The pore size distribution was determined by applying the QSDFT technique and density



functional theory (DFT). The total pore volume was measured from the adsorption isotherm by assessing nitrogen adsorption at a relative pressure of  $p/p_0 = 0.99$ . All computations were conducted using the Quantachrome-developed ASiQwin application (Version 2.0).

## 2.2. Characterization of Wastewater Used for Adsorption Studies

Two filtration experiments were carried out using wastewater obtained from an operational individual wastewater treatment plant. Approximately  $100 \pm 10$  L of wastewater from the wastewater treatment plant was poured into the tank (Figure 3). This wastewater had already been biologically treated. The main pollution indicators of wastewater (after biological treatment) are presented in Table 1.

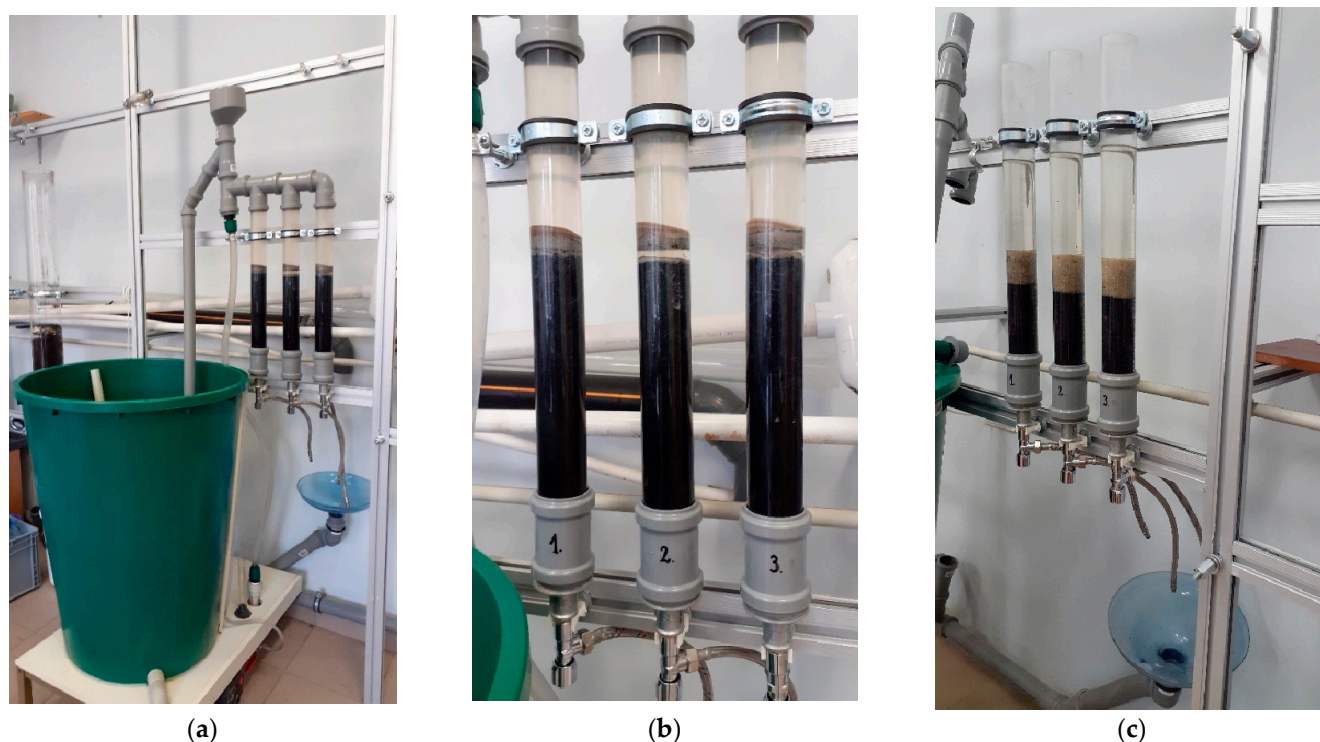


**Figure 3.** Experimental set-up: (a)—general view; (b)—experiment No. 1; (c)—experiment No. 2. Column No. 1—contains PS\_400 filler, column No. 2—PS\_500 filler, column No. 3—PS\_600 filler.

**Table 1.** Average initial indicators of pollution of wastewater used in the study.

Indicator	COD (mg/L)	BOD <sub>7</sub> (mg/L)	SS (mg/L)	NO <sub>3</sub> -N (mg/L)	NH <sub>4</sub> -N (mg/L)	PO <sub>4</sub> -P (mg/L)	pH
			Experiment No. 1				
Value	41	9.6	10.1	5.53	10.64	1.38	7.5
			Experiment No. 2				
Value	39	7.5	8.6	9.45	8.33	3.93	7.6

As indicated in Table 1, wastewater contained only small concentrations of chemical oxygen demand (COD), biological oxygen demand (BOD<sub>7</sub>), and suspended solids (SS). The presence of a small amount (9–10 mg/L) of SS in wastewater is unlikely to cause the clogging of filter columns in laboratory tests, as previously observed [33]. The wastewater used in the study had a neutral pH. Furthermore, the concentrations of ammonium nitrogen (NH<sub>4</sub>-N) and nitrates (NO<sub>3</sub>-N) in the wastewater were low. PO<sub>4</sub>-P concentrations in wastewater handled by specific wastewater treatment plants vary a lot, so for experiment No. 1, the concentration was raised to the highest value that is typically seen (25–30 mg/L). The concentration of PO<sub>4</sub>-P in the solution was increased by adding K<sub>2</sub>HPO<sub>4</sub> (experiment

No. 1). This salt was thoroughly mixed and dissolved, first in a small amount of wastewater and then in the entire wastewater tank. Experiment No. 2 was carried out using real wastewater, in which the concentration of  $\text{PO}_4\text{-P}$  was 3.93 mg/L. This concentration was not increased by the addition of  $\text{K}_2\text{HPO}_4$ .

### 2.3. Experimental Design

An experimental filtration set-up with columns was installed in the laboratory of VILNIUS TECH, as shown in Figure 3.

Biologically treated wastewater (104 L) was transferred to a tank (Figure 3), from which it was pumped through a distribution pipe to three filtration columns. Filtration was performed daily for 12 h, during which 34 L of effluent flowed from each column. The experiments were carried out at room temperature (approx. 20 °C). No filtration was performed at night. The wastewater was filtered at a flow rate of 8 mL/min. Pyrolyzed sludge particles were poured onto a support bed of fine stones in three filtration columns. Sewage sludge biochar pyrolyzed at temperatures of 400 °C, 500 °C, and 600 °C with particle sizes between 1.0 and 1.6 mm (experiment No. 1) and 0.6 and 1.0 mm (experiment No. 2) were used to fill the columns. Detailed parameters of the filter media are provided in Table 2.

**Table 2.** Parameters of different adsorbent media.

Column No.	Pyrolysis Temperature, °C	Fraction, mm	Volume, mL	Column Height, cm	Mass, g	Apparent Density, (g/cm <sup>3</sup> )
Experiment No. 1						
1	400	1.0–1.6	400	27.2	208	0.520
2	500	1.0–1.6	400	27.2	211	0.528
3	600	1.0–1.6	400	27.2	209	0.523
Experiment No. 2						
1	400	0.6–1.0	200	13.6	130	0.650
2	500	0.6–1.0	200	13.6	131	0.645
3	600	0.6–1.0	200	13.6	128	0.639

In experiment No. 1, the column media was covered using a mesh, whereas in experiment No. 2, a 5 cm layer of sand was applied over the biochar media. Identically sized columns with a diameter of 4.5 cm were employed in both experiments. For each experiment (No. 1 and No. 2), all three columns were uniformly packed with sewage sludge biochar of the identical fraction, as detailed in Table 3. It is important to note that pristine sewage sludge biochar was introduced into each column.

**Table 3.** Specific surface area ( $S_{\text{BET}}$ ), micropore area ( $S_{\text{mic}}$ ), external surface area ( $S_{\text{ext}}$ ), pore volume ( $V_{\text{p}}$ ), average pore size (APS), and porosity ( $\epsilon$ ) of pyrolyzed sewage sludge.

Sample Code	$S_{\text{BET}}$ , m <sup>2</sup> /g	$S_{\text{mic}}$ , m <sup>2</sup> /g	$S_{\text{ext}}$ , m <sup>2</sup> /g	$V_{\text{pore}}$ , mL/g	APS, nm	$\epsilon$
PS_400 (2)	127.589	94.2	33.389	0.090	5.39	0.979
PS_500 (3)	82.669	54.7	27.969	0.074	6.92	0.975
PS_600 (4)	107.994	67.3	40.694	0.095	5.60	0.980

Throughout the experiments, the filter media were fully submerged, filtering from top to bottom. Filtrate samples were taken from all columns simultaneously at predetermined time intervals. At the same time, samples of wastewater were taken from the tank. The samples were analyzed in the laboratory.  $\text{PO}_4\text{-P}$  concentrations were measured using MERCK Spectroquant<sup>®</sup> (Darmstadt, Germany) assays. Test samples were placed in cuvettes (Hellma, MERCK, Darmstadt, Germany) and measured for absorbance at the necessary wavelength using a Genesys 10 UV-Vis spectrophotometer (Thermo Fisher Scientific, Waltham, MA, USA). Each sample underwent three tests, and the average results were recorded. The values of the indices differed by 6–12%. The pH was determined potentiometrically, measured with a WTW pH-meter pH-330i, and reference buffer solutions

certified by Hamilton from Carl Roth GmbH+ Co. KG (Karlsruhe, Germany) were used for the quality control of measurements.

The efficiency of the removal of PO<sub>4</sub>-P ( $E_i$ , %) from the solution in each column was calculated according to the following Formula (1):

$$E_i = (C_0 - C_i) \times 100 / C_0, \quad (1)$$

where  $C_0$  was PO<sub>4</sub>-P concentration before filtration (mg/L) and  $C_i$  was PO<sub>4</sub>-P concentration after filtration, (mg/L).

### 3. Results and Discussion

#### 3.1. Surface Area and Porosity

The nitrogen adsorption–desorption isotherms (Figure 4) were used for calculating the surface area and conducting an in-depth analysis of the pore characteristics of pyrolyzed sludge. The shapes of all isotherms and the configuration of their hysteresis loops made it possible to refer to them as type IV with H3-type hysteresis loops (IUPAC) [34]. Consequently, it can be concluded that all samples could be classed as mesoporous materials with a high adsorption performance. The H3 hysteresis loop indicates the presence of non-rigid aggregates with slit-like pores.

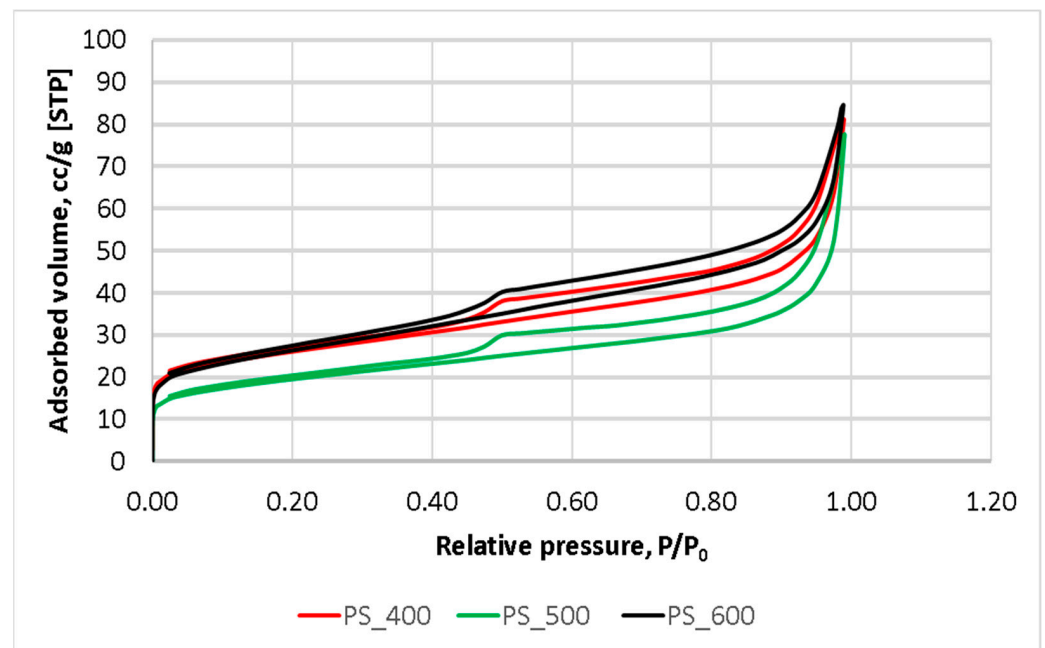


Figure 4. N<sub>2</sub> adsorption–desorption isotherms.

The main structural characteristics of the samples, including BET surface area ( $S_{\text{BET}}$ ), micropore area ( $S_{\text{micro}}$ ), external area ( $S_{\text{ext}}$ ), pore volume ( $V_{\text{pore}}$ ), and average pore size (APS), along with porosity, are displayed in Table 3.

The porosity of the particles ( $\epsilon$ ) was calculated using the following Equation (2):

$$\epsilon = V_p / (V_p + 1 / \rho_{\text{app}}), \quad (2)$$

where  $V_p$  is the pore volume (cm<sup>3</sup>/g), and  $\rho_{\text{app}}$  is the apparent density (g/cm<sup>3</sup>) of the material.

As can be seen from Table 3, the specific surface area of the samples decreased when the pyrolysis temperature was increased up to 500 °C and then began to increase. This is due to the effect of the activation temperature on the physical characteristics of biochar. As described in [35], the specific surface area of the samples depends on the carbonization temperature and reaches its maximum at 600–700 °C. A gradual decrease in the specific

surface area, micropores, and external surface area of the samples, with a simultaneous increase in the average pore size when heated to 400 and 500 °C, possibly indicating sintering, was observed. However, at 600 °C, the sewage sludge biochar was already reaching a carbonized state, and its specific surface area had begun to increase. At the same time, the surface of the mesopores increased by 45% and the micropores by only 23%. The pore volume reached the value of 0.095 mL/g, and the porosity rose. An interesting fact is that, during pyrolysis at 600 °C, the specific surface area of the sample remained lower than it was at 400 °C, but the surface area of the mesopores increased, contributing to the increase in the adsorption potential of the sample.

As in Figure 5, pyrolysis at 400 and 500 °C resulted in a reduction in the volume of pores of 2–39 nm. Additionally, pyrolysis at 600 °C led to an increase in the volume of pores in the range of 2–15 nm and the appearance of new pores in the range of 36–50 nm. Thus, the pyrolysis of sewage sludge at a temperature of 600 °C and above makes it possible to predict an enhancement of its sorption properties.

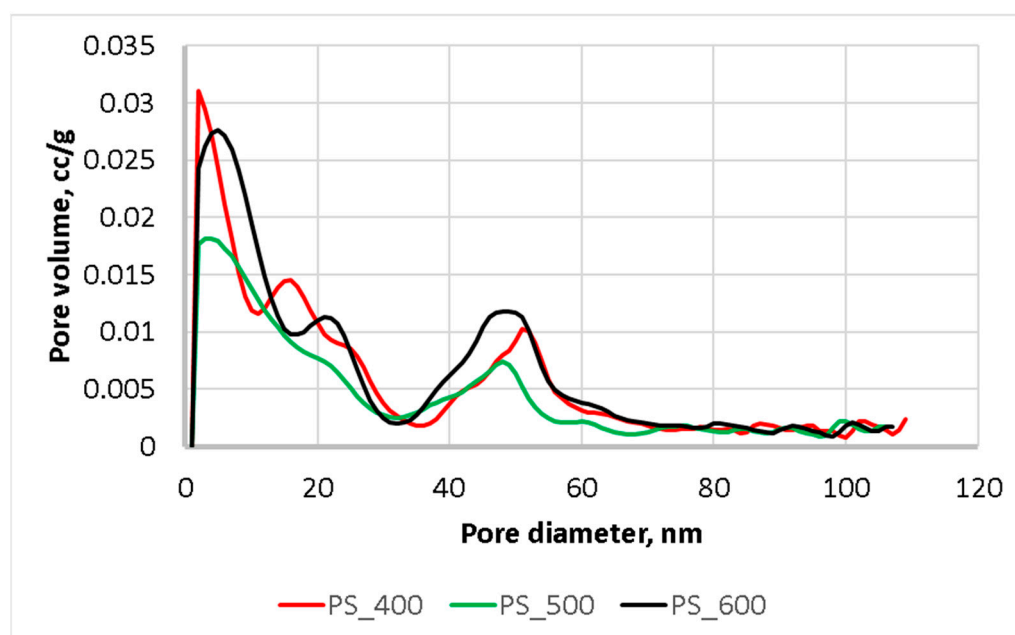


**Figure 5.** Pore size distribution.

### 3.2. Results of the Filtration Experiments

The results of experiment No. 1 are shown in Figure 6. When filtering wastewater at a rate of 8 mL/min, its residence time in the columns was 50 min. Figure 6 shows that during the first hour of filtration, PO<sub>4</sub>-P was retained most effectively by the third column containing sewage sludge pyrolyzed at 600 °C (efficiency 87%). The least efficient (efficiency 31%) result was from the first column filled with sewage sludge pyrolyzed at 400 °C. From the results presented in Figure 6, it can be seen that the PO<sub>4</sub>-P retention efficiency of all filter media decreased to 30–40% during the first 17 h of filtration and did not change significantly thereafter (17–42 h of filtration). At the end of the experiment, the efficiency of all three columns was still at least 30%. It was observed that, after 42 h of filtration, a slimy layer of sediment appeared above the filter media on the grids (Figure 3b). The sediment that accumulated on the surface of the column media came from the filtered wastewater, which contained small amounts of suspended solids and organic matter (Table 1). This sediment layer could contribute to PO<sub>4</sub>-P retention, so even after 42 h of filtration, the PO<sub>4</sub>-P retention efficiency was positive.

Experiment No. 2 was performed by filtering wastewater with a lower initial PO<sub>4</sub>-P concentration (3.93 mg/L). Biochar particles were pressed with a 5 cm high layer of quartz sand (Figure 3c).



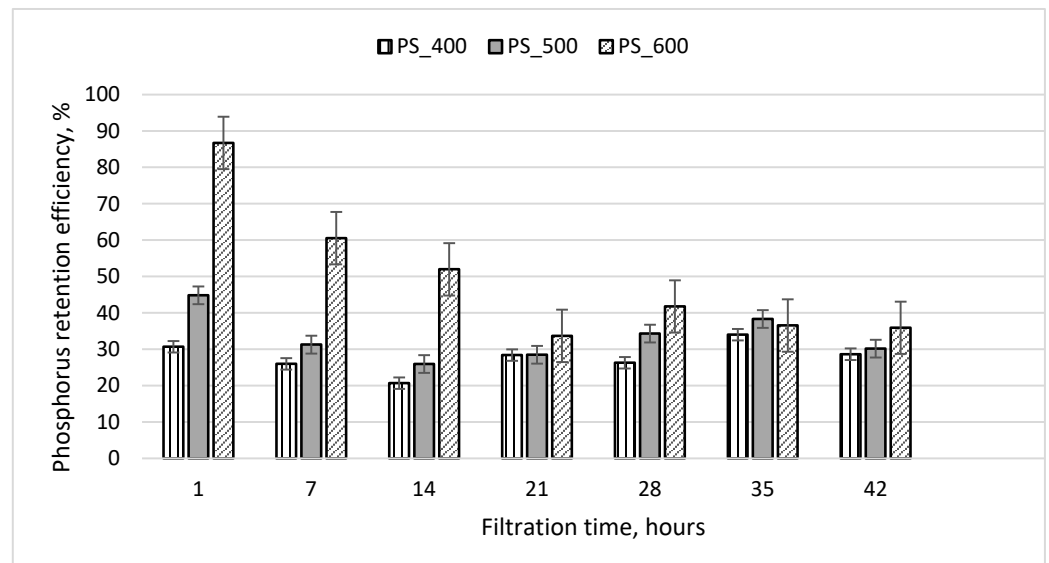


**Figure 6.** Phosphorus retention efficiency during experiment No. 1. The initial concentration of  $\text{PO}_4\text{-P}$  in the wastewater was 25.5 mg/L; the initial weight of pyrolyzed sludge inside the column was 209 g; the particle size was 1.0–1.6 mm.

The results of experiment No. 2 are presented in Figure 7. During this experiment, the initial  $\text{PO}_4\text{-P}$  concentration of treated wastewater was six times lower, and the residence time of the wastewater in the column media was two times lower than in experiment No. 1. During the first 1.5 h of filtration,  $\text{PO}_4\text{-P}$  was retained most effectively by the third column, which contained sewage sludge pyrolyzed at a temperature of 600 °C (retention efficiency of 78%). The  $\text{PO}_4\text{-P}$  retention efficiency in the second column initially reached 21%, and after 5 h, it was 0%. The effluent from the first column always contained the same concentration of  $\text{PO}_4\text{-P}$  as the initial concentration found in the wastewater. It is concluded that the media in the first column did not retain phosphorus. This finding was influenced by the insufficient residence time of the treated wastewater in the column media (25 min). According to Mekonnen et al. (2020), increasing the contact time increases phosphate uptake, indicating a rapid filling of active sites due to boundary layer diffusion [36].

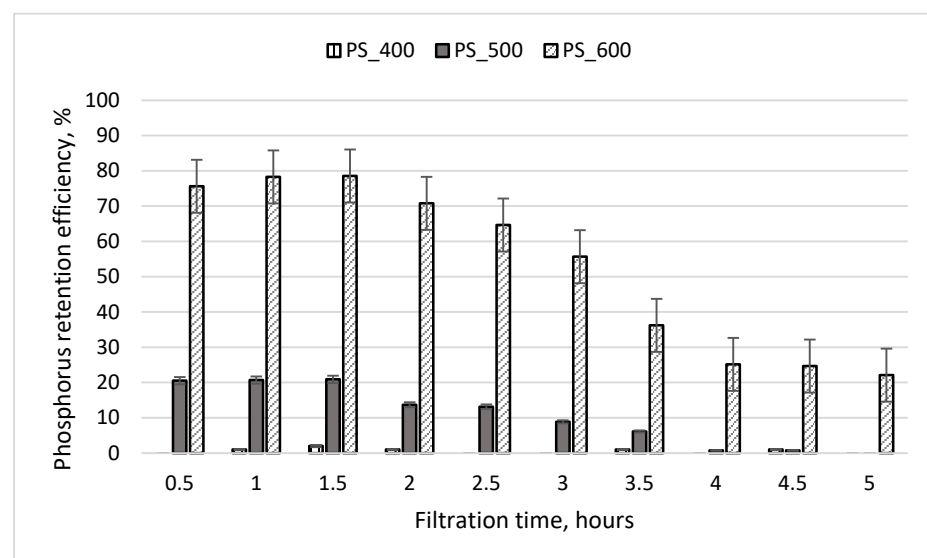


**Figure 7.** Phosphorus retention efficiency during experiment No. 2. The initial concentration of  $\text{PO}_4\text{-P}$  in the wastewater was 3.93 mg/L; the initial weight of pyrolyzed sludge inside the column was 130 g; the particle size was 0.6–1.0 mm.

In both experiments, the  $\text{PO}_4\text{-P}$  removal efficiency from wastewater was lowest with PS\_400 column media and highest with PS\_600 column media. Two filtration experiments, conducted at a flow rate of 8 mL/min, revealed that the column containing sewage sludge pyrolyzed at 600 °C exhibited the most effective  $\text{PO}_4\text{-P}$  retention during the first and second experiments, with retention efficiencies of 87% and 78%, respectively, obtained after 1 h of filtration. This result is due to the composition of pyrolyzed sewage sludge (Figure 2). PS\_600 samples contained the highest concentration of Mg, Al, Si, K, Ca, Fe, and Zn. Metals are known to adsorb phosphorus through chemisorption [37]. According to Pugliese et al., Fe can attract and retain phosphorus [38]. According to Adly et al. (2022), activated carbon does not remove phosphorus from water, but when coated with nanoscale iron particles, it attracts phosphorus and forms complexes between Fe oxides and phosphorus (P–O–Fe) as a chemisorption process takes place [39]. The process can change if the pH changes, as Fe dissolves at high or low pH values. A pH range of 7 to 8 is favorable for phosphorus adsorption, as Fe is insoluble under these conditions [39]. The conditions of this study were appropriate for the formation of complexes between Fe and phosphorus since the pH of the wastewater was 7.5–7.6.

Measuring the pH of the filtrates from the columns revealed that it was higher than the initial pH of the wastewater. During both experiments, the pH of the filtrates increased in the following order: in the first column by 3–4%, in the second column by 5–7%, and in the third column by 15–18%. The pH of the wastewater was likely to increase because the pyrolysis of sewage sludge at 600 °C increased the concentration of alkali metals in it [39]. Therefore, the higher the temperature of the pyrolyzed sludge, the higher its pH. Previously, Januševičius et al. (2024) observed that as the sludge pyrolysis temperature increased from 400 °C to 600 °C, the concentrations of Ca, Mg, and K in biochar increased by 9, 3, and 11.5%, respectively [30].  $\text{PO}_4\text{-P}$  adsorption onto the biochar was shown to be greatly aided by the concentrations of Ca and Mg [11,39]. Numerous studies have investigated the effect of pyrolysis temperature on phosphate adsorption by biochar. However, there is no agreement regarding the ideal synthesis temperature, as it is highly influenced by the specific raw materials used [11]. Before producing biochar, it is essential to subject organic waste to anaerobic digestion. Yao et al. (2011) observed that after the anaerobic digestion of sugar beet tailings, followed by pyrolysis at 600 °C, the resulting biochar demonstrated significantly improved phosphate adsorption capacities. This enhancement was attributed to the development of a mesoporous structure, a larger surface area, and a higher zeta potential [40]. The biochar used in this study was derived from anaerobically digested sewage sludge that had been subjected to a thermohydrolysis process. This technological process could increase the volume of biochar pores and the surface area of the mesopores. Biochar is gaining much interest in the wastewater treatment industry because of its high porosity, large surface area, rich surface functional groups, and high pH value [41]. A positive feature of biochar is that it does not pollute the water itself. Our previous study showed that Zn, Cu, Cr, Mn, Ni, and Pb were not leached from sewage sludge biochar produced at a temperature of 600 °C [30]. Although the materials and production processes used to make biochar and activated carbon are identical, biochar is produced at a lower temperature than activated carbon, which results in a price that is one-sixth of that of commercial activated carbon [42]. On the other hand, sewage sludge is a waste product, and its amount should be reduced, thus contributing to the development of environmental sustainability.

#### 4. Conclusions

This work investigated the adsorption properties of pyrolyzed sewage sludge at different temperatures (400, 500, and 600 °C) and the efficiency of removing  $\text{PO}_4\text{-P}$  from wastewater by filtration. Nitrogen adsorption–desorption isotherms were used for calculating the surface area and undertaking an in-depth analysis of the pore characteristics of pyrolyzed sludge. The BET surface area and pore size distribution were determined. Based on the results, it can be concluded that all samples could be categorized as mesoporous

materials with a high adsorption performance. During pyrolysis at 600 °C, the specific surface area of the sample remained lower than it was at 400 °C, but the surface area of the mesopores increased, contributing to the increase in the adsorption potential of the sample.

Two wastewater filtration experiments (at a rate of 8 mL/min) using three columns filled with sewage sludge pyrolyzed at temperatures of 400, 500, and 600 °C were carried out. The size of the media fraction was 1.0–1.6 mm in the first experiment and 0.6–1.0 mm in the second experiment. The tests were carried out with real biologically treated wastewater with a PO<sub>4</sub>-P concentration of 1.4–4.0 mg/L. The concentration of PO<sub>4</sub>-P in the wastewater treated by individual wastewater treatment plants varies greatly, so it was increased to the maximum that actually occurs (25–30 mg/L) during the first filtration experiment. The efficiency of PO<sub>4</sub>-P removal from wastewater varied depending on the filter column media and the residence time of the wastewater in the column. The experiments showed that the first column (filled with sewage sludge pyrolyzed at 400 °C) did not retain PO<sub>4</sub>-P due to the smaller surface area of the mesopores. The third column, which contained sewage sludge pyrolyzed at 600 °C, retained PO<sub>4</sub>-P most effectively during the first and second experiments (87 and 78% retention efficiency, respectively). The pyrolysis of sewage sludge at 600 °C increased the concentration of alkali metals, which makes PO<sub>4</sub>-P sorption more efficient. Overall, the study data provide valuable insights into the effectiveness of pyrolyzed (400–600 °C) sewage sludge in removing phosphorus from wastewater. However, further research is needed to determine the optimal conditions for phosphorus removal and to develop more effective and sustainable methods for treating wastewater.

**Author Contributions:** Conceptualization, T.J., A.M., K.S. and D.P.; methodology, T.J., A.M. and D.P.; validation, V.D. and D.P.; formal analysis, A.M., K.S. and D.P.; investigation, T.J., A.M. and K.S.; resources, T.J., K.S. and V.D.; data curation, T.J., A.M. and D.P.; writing—original draft preparation, T.J., A.M., K.S. and V.D.; writing—review and editing, A.M., K.S. and V.D.; visualization, A.M. and K.S.; supervision, T.J. and A.M. All authors have read and agreed to the published version of the manuscript.

**Funding:** Research was conducted as part of the execution of Project “Mission-driven Implementation of Science and Innovation Programmes” (No. 02-002-P-0001), funded by the Economic Revitalization and Resilience Enhancement Plan “New Generation Lithuania”.

**Data Availability Statement:** Data are contained within the article.

**Conflicts of Interest:** The authors declare no conflicts of interest.

## References

1. Geng, H.; Xu, Y.; Zheng, L.; Gong, H.; Dai, L.; Dai, X. An overview of removing heavy metals from sewage sludge: Achievements and perspectives. *Environ. Pollut.* **2020**, *266*, 115375. [[CrossRef](#)] [[PubMed](#)]
2. Agoro, M.A.; Adeniji, A.O.; Adefisoye, M.A.; Okoh, O.O. Heavy Metals in Wastewater and Sewage Sludge from Selected Municipal Treatment Plants in Eastern Cape Province, South Africa. *Water* **2020**, *12*, 2746. [[CrossRef](#)]
3. Wojciula, A.; Boruszko, D.; Pajewska, G. Analysis of Heavy Metal Fraction Content in Sewage Sludge from Selected Wastewater Treatment Plants. *J. Ecol. Eng.* **2021**, *22*, 98–105. [[CrossRef](#)]
4. Kowalik, R.; Gawdzik, J.; Bąk-Patyna, P.; Ramiączek, P.; Jurišević, N. Risk Analysis of Heavy Metals Migration from Sewage Sludge of Wastewater Treatment Plants. *Int. J. Environ. Res. Public Health* **2022**, *19*, 11829. [[CrossRef](#)] [[PubMed](#)]
5. Ali, H.; Khan, E.; Ilahi, I. Environmental Chemistry and Ecotoxicology of Hazardous Heavy Metals: Environmental Persistence, Toxicity, and Bioaccumulation. *J. Chem.* **2019**, *2019*, 6730305. [[CrossRef](#)]
6. Seshadri, B.; Bolan, N.S.; Choppala, G.; Kunhikrishnan, A.; Sanderson, P.; Wang, H.; Currie, L.D.; Tsang, D.C.W.; Ok, Y.S.; Kim, G. Potential value of phosphate compounds in enhancing immobilization and reducing bioavailability of mixed heavy metal contaminants in shooting range soil. *Chemosphere* **2017**, *184*, 197–206. [[CrossRef](#)] [[PubMed](#)]
7. Andrunik, M.; Wołowicz, M.; Wojnarski, D.; Zelek-Pogudź, S.; Bajda, T. Transformation of Pb, Cd, and Zn Minerals Using Phosphates. *Minerals* **2020**, *10*, 342. [[CrossRef](#)]
8. Comber, S.; Gardner, M.; Darmovzalova, J.; Ellor, B. Determination of the forms and stability of phosphorus in wastewater effluent from a variety of treatment processes. *J. Environ. Chem. Eng.* **2015**, *3*, 2924–2930. [[CrossRef](#)]
9. Zhang, Y.; Yang, K.; Fang, Y.; Ding, J.; Zhang, H. Removal of Phosphate from Wastewater with a Recyclable La-Based Particulate Adsorbent in a Small-Scale Reactor. *Water* **2022**, *14*, 2326. [[CrossRef](#)]



10. Usman, M.; Aturagaba, G.; Ntale, M.; Nyakairu, G. A review of adsorption techniques for removal of phosphates from wastewater. *Water Sci. Technol.* **2022**, *86*, 3113–3132. [[CrossRef](#)]
11. Nobaharan, K.; Bagheri Novair, S.; Asgari Lajayer, B.; van Hullebusch, E.D. Phosphorus Removal from Wastewater: The Potential Use of Biochar and the Key Controlling Factors. *Water* **2021**, *13*, 517. [[CrossRef](#)]
12. Bunce, J.T.; Ndam, E.; Ofiteru, I.D.; Moore, A.; Graham, D.W. A Review of Phosphorus Removal Technologies and Their Applicability to Small-Scale Domestic Wastewater Treatment Systems. *Front. Environ. Sci.* **2018**, *6*, 8. [[CrossRef](#)]
13. Li, Y.; Nan, X.; Li, D.; Wang, L.; Xu, R.; Li, Q. Advances in the treatment of phosphorus-containing wastewater. *IOP Conf. Ser. Earth Environ. Sci.* **2021**, *647*, 012163. [[CrossRef](#)]
14. Yu, S.; Liu, S.; Yao, X.; Ning, P. Enhanced biological phosphorus removal from wastewater by current stimulation coupled with anaerobic digestion. *Chemosphere* **2022**, *293*, 133661. [[CrossRef](#)]
15. Zheng, Y.; Wan, Y.; Zhang, Y.; Huang, J.; Yang, Y.; Tsang, D.C.W.; Wang, H.; Chen, H.; Gao, B. Recovery of phosphorus from wastewater: A review based on current phosphorous removal technologies. *Crit. Rev. Environ. Sci. Technol.* **2022**, *53*, 1148–1172. [[CrossRef](#)]
16. Almanassra, I.; McKay, G.; Kochkodan, V.; Atieh, M.; Al-Ansari, T.A. State of the art review on phosphate removal from water by biochars. *J. Chem. Eng.* **2021**, *409*, 128211. [[CrossRef](#)]
17. Yang, Z.; Zhou, Y.; Feng, Z.; Rui, X.; Zhang, T.; Zhang, Z. A Review on Reverse Osmosis and Nanofiltration Membranes for Water Purification. *Polymers* **2019**, *11*, 1252. [[CrossRef](#)] [[PubMed](#)]
18. Cairns, S.; Robertson, I.; Sigmund, G.; Street-Perrott, A. The removal of lead, copper, zinc and cadmium from aqueous solution by biochar and amended biochars. *Environ. Sci. Pollut. Res. Int.* **2020**, *27*, 21702–21715. [[CrossRef](#)]
19. Wang, P.; Zhi, M.; Cui, G.; Chu, Z.; Wang, S.A. comparative study on phosphate removal from water using Phragmites australis biochars loaded with different metal oxides. *R. Soc. Open Sci.* **2021**, *8*, 201789. [[CrossRef](#)]
20. Feng, Y.; Zhao, D.; Qiu, S.; He, Q.; Luo, Y.; Zhang, K.; Shen, S.; Wang, F. Adsorption of Phosphate in Aqueous Phase by Biochar Prepared from Sheep Manure and Modified by Oyster Shells. *ACS Omega* **2021**, *6*, 33046–33056. [[CrossRef](#)]
21. Zhang, C.h.; Sun, S.; Xu, S.; Johnston, C.; Wu, C. Phosphorus Removal from Dirty Farmyard Water by Activated Anaerobic-Digestion-Derived Biochar. *Ind. Eng. Chem. Res.* **2022**, *62*, 19216–19224. [[CrossRef](#)]
22. Mahdi, Z.; Yu, Q.J.; El Hanandeh, A. Competitive adsorption of heavy metal ions (Pb<sup>2+</sup>, Cu<sup>2+</sup>, and Ni<sup>2+</sup>) onto date seed biochar: Batch and fixed bed experiments. *Sep. Sci.* **2019**, *54*, 888–901. [[CrossRef](#)]
23. Zhao, M.; Dai, Y.; Zhang, M.; Feng, C.; Qin, B.; Zhang, W.; Zhao, N.; Li, Y.; Ni, Z.; Xu, Z.; et al. Mechanisms of Pb and/or Zn adsorption by different biochars: Biochar characteristics, stability, and binding energies. *Sci. Total Environ.* **2020**, *717*, 136894. [[CrossRef](#)]
24. Yang, L.; He, L.; Xue, J.; Wu, L.; Ma, Y.; Li, H.; Peng, P.; Li, M.; Zhang, Z. Highly efficient nickel (II) removal by sewage sludge biochar supported  $\alpha$ -Fe<sub>2</sub>O<sub>3</sub> and  $\alpha$ -FeOOH: Sorption characteristics and mechanisms. *PLoS ONE* **2019**, *14*, e218114. [[CrossRef](#)]
25. Fan, L.; Wang, X.; Miao, J.; Liu, Q.; Cai, J.; An, X.; Chen, F.; Cheng, L.; Chen, W.; Luo, H.; et al. Na<sub>4</sub>P<sub>2</sub>O<sub>7</sub>-Modified Biochar Derived from Sewage Sludge: Effective Cu(II)-Adsorption Removal from Aqueous Solution. *Adsorp. Sci. Technol.* **2023**, *2023*, 8217910. [[CrossRef](#)]
26. Rio, S.; Faur-Brasquet, C.; Le Coq, L.; Le Cloirec, P. Structure characterization and adsorption properties of pyrolyzed sewage sludge. *Environ. Sci. Technol.* **2005**, *39*, 4249–4257. [[CrossRef](#)]
27. Zielińska, A.; Oleszczuk, P. Evaluation of sewage sludge and slow pyrolyzed sewage sludge-derived biochar for adsorption of phenanthrene and pyrene. *Bioresour. Technol.* **2015**, *192*, 618–626. [[CrossRef](#)] [[PubMed](#)]
28. Xu, Q.; Tang, S.; Wang, J.; Ko, J.H. Pyrolysis kinetics of sewage sludge and its biochar characteristics. *Process Saf. Environ. Prot.* **2018**, *115*, 49–56. [[CrossRef](#)]
29. Wang, L.; Zhao, Y.; Li, Y.; Yao, B.; Zhang, C.H.; Zhang, W.; Niu, L.; Zhang, H. Fe-loaded biochar facilitates simultaneous bisphenol A biodegradation and efficient nitrate reduction: Physicochemical properties and biological mechanism. *J. Clean. Prod.* **2022**, *372*, 133814. [[CrossRef](#)]
30. Januševičius, T.; Mažeikienė, A.; Danila, V.; Paliulis, D. The characteristics of sewage sludge pellet biochar prepared using two different pyrolysis methods, Biomass conversion and biorefinery. *Biomass Convers. Biorefin.* **2024**, *14*, 891–900. [[CrossRef](#)]
31. Takaya, C.; Fletcher, L.; Singh, S.; Anyikude, K.; Ross, A. Phosphate and ammonium sorption capacity of biochar and hydrochar from different wastes. *Chemosphere* **2016**, *145*, 518–527. [[CrossRef](#)] [[PubMed](#)]
32. Sarkhot, D.V.; Ghezzehei, T.A.; Berhe, A.A. Effectiveness of biochar for sorption of ammonium and phosphate from dairy effluent. *J. Environ. Qual.* **2013**, *42*, 1545–1554. [[CrossRef](#)] [[PubMed](#)]
33. Mažeikienė, A.; Vaiškūnaitė, R.; Šarko, J. Sand from groundwater treatment coated with iron and manganese used for phosphorus removal from wastewater. *Sci. Total Environ.* **2021**, *764*, 142915. [[CrossRef](#)] [[PubMed](#)]
34. Thommes, M.; Kaneko, K.; Neimark, A.V.; Olivier, J.P.; Rodriguez-Reinoso, F.; Rouquerol, J.; Sing, K.S.W. Physisorption of 516 gases, with special reference to the evaluation of surface area and pore size distribution (IUPAC Technical Report). *Pure Appl. Chem.* **2015**, *87*, 1051–1069. [[CrossRef](#)]
35. Kwon, S.H.; Lee, E.; Kim, B.S.; Kim, S.-G.; Lee, B.-J.; Kim, M.-S.; Jung, J.C. Preparation of activated carbon aerogel and its application to electrode material for electric double layer capacitor in organic electrolyte: Effect of activation temperature. *Korean J. Chem. Eng.* **2015**, *32*, 248–254. [[CrossRef](#)]

36. Mekonnen, D.T.; Alemayehu, E.; Lennartz, B. Removal of Phosphate Ions from Aqueous Solutions by Adsorption onto Leftover Coal. *Water* **2020**, *12*, 1381. [[CrossRef](#)]
37. Gubernat, S.; Masłóń, A.; Czarnota, J.; Koszelnik, P. Reactive Materials in the Removal of Phosphorus Compounds from Wastewater-A Review. *Materials* **2020**, *13*, 3377. [[CrossRef](#)]
38. Pugliese, L.; Canga, E.; Hansen, H.; Kjærgaard, C.H.; Heckrath, G.; Poulsen, T. Long-term phosphorus removal by Ca and Fe-rich drainage filter materials under variable flow and inlet concentrations. *Water Res.* **2023**, *247*, 120792. [[CrossRef](#)] [[PubMed](#)]
39. Veni, D.K.; Kannan, P.; Edison, T.N.; Senthilkumar, A. Biochar from green waste for phosphate removal with subsequent disposal. *Waste Manag.* **2017**, *68*, 752–759. [[CrossRef](#)]
40. Yao, Y.; Gao, B.; Inyang, M.; Zimmerman, A.R.; Cao, X.; Pullammanappallil, P.; Yang, L. Removal of phosphate from aqueous solution by biochar derived from anaerobically digested sugar beet tailings. *J. Hazard. Mater.* **2011**, *190*, 501–507. [[CrossRef](#)]
41. Ahmad, M.; Rajapaksha, A.U.; Lim, J.E.; Zhang, M.; Bolan, N.; Mohan, D.; Vithanage, M.; Lee, S.S.; Ok, Y.S. Biochar as a sorbent for contaminant management in soil and water: A review. *Chemosphere* **2014**, *99*, 19–33. [[CrossRef](#)] [[PubMed](#)]
42. Zhang, X.; Gao, B.; Creamer, A.E.; Cao, C.; Li, Y. Adsorption of VOCs onto engineered carbon materials: A review. *J. Hazard. Mater.* **2017**, *338*, 102–123. [[CrossRef](#)] [[PubMed](#)]

**Disclaimer/Publisher’s Note:** The statements, opinions and data contained in all publications are solely those of the individual author(s) and contributor(s) and not of MDPI and/or the editor(s). MDPI and/or the editor(s) disclaim responsibility for any injury to people or property resulting from any ideas, methods, instructions or products referred to in the content.